Theoretical Gain Optimization Studies in 16-μm CO_2-N_2-H_2 Gasdynamic Lasers

N. M. Reddy* and K.P.J. Reddy†
Indian Institute of Science, Bangalore, India

The governing equations for gas flows in 16-μm CO_2-N_2-H_2 gasdynamic lasers using conical or hyperbolic nozzles have been presented in universal form so that for a given gas composition the solutions depend on a single parameter that combines all other parameters of the laser system. The solutions of these equations are used to compute the optimum values of small signal optical gain, and the corresponding optimum values of the area ratio, the reservoir temperature T_0' and the binary scaling parameter $p_0'L'$, which is a product of reservoir pressure p_0' and nozzle shape factor L', for a wide range of gas mixture compositions. The results are presented in graph form. An optimum value of 2.06% cm^{-1} gain has been calculated for the gas composition of CO_2:N_2:H_2 = 15:65:20.

Nomenclature

A	= local cross-sectional area of the nozzle
B,J	= constants
$\bar{E}_{\rm I},\bar{E}_{\rm II}$	= functions defined in Eqs. (16)
e	= specific energy
$\bar{G}_{\rm I},\bar{G}_{\rm II}$	= functions defined in Eqs. (17)
G_0	= small signal gain
i,j	= indices controlling the nozzle shape
$K_{\rm I},K_{\rm II},K_a,K_b$	= functions defined in Eqs. (18) and (19)
k_1,k_2	= functions defined in Eqs. (23) and (24)
L'	= reference length (nozzle shape parameter = $r_*'/\tan\delta$)
M	= Mach number
N	= particle or species number density
N_s	= nonsimilar function defined in Eq. (21)
P	= function defined in Eq. (13)
p'	= pressure
Q	= partition function
R'	= mixture gas constant per unit mass
r_*'	= throat radius
S	= specific entropy
T'	= absolute temperature
u'	= velocity
X	= mole fraction
x'	= distance in the flow direction
α	= factor defined in Eq. (6b)
δ	= semiexpansion angle of the conical nozzle or semiasymptotic cone angle of a hyperbolic nozzle
θ	= characteristic vibrational temperature
ξ	= independent variable
ρ	= density
τ_a',τ_b',τ_c'	= average relaxation times
$\phi_{\rm I},\phi_{\rm II}$	= normalized vibrational temperatures
$\chi_{\rm I},\chi_{\rm II}$	= parameters defined in Eqs. (20)
ψ	= normalized translational temperature

Subscripts

C	= carbon dioxide
e	= equilibrium value
H	= hydrogen
M	= mixture
N	= nitrogen
opt	= optimum value
v	= vibrational level
ν_1,ν_2,ν_3	= vibrational modes of CO_2
$\nu_{\rm N}$	= vibrational mode of N_2
I,II	= modes I and II
0	= reservoir condition
( )*	= throat condition
(02^{0}0),(001)	= corresponding to levels (02^{0}0) and (001)

Introduction

THE possibility of laser isotope separation has spurred a rather substantial effort toward the generation of molecular lasers operating in the wavelength regions of UF_6 absorption. Recently, 16-μm lasers have been found to be potential light sources for uranium isotope separation. Therefore, much effort has been exerted to develop new 16-μm lasers. Osgood[1] used a HBr laser to excite the HBr in the CO_2-HBr mixture which, in turn, excited CO_2 molecules to the (001) level (Fig. 1). The 16-μm operation was achieved using a 9.6-μm stimulant which depleted the population of the (001) level to the (020) level, thus creating the population inversion between the (020) and (010) levels of the CO_2 molecules. Tiee and Witling[2] used a simple optical pumping technique which employed a CO_2 TEA laser to obtain 4 and 3 mJ/pulse from CF_4 and NOCl, respectively, in the 16-μm region. Baranov et al.[3] obtained a maximum average power of 200 mW at 60 Hz in a CF_4 laser. Byer[4] proposed and demonstrated for the first time the 16-μm H_2 Raman laser by means of Raman shifting the 10.6-μm output from a CO_2 laser to 16-μm. Remarkably high quantum efficiency from the H_2 Raman laser was realized by Rabinowitz et al.,[5] where an output energy in excess of 1 J/pulse and a peak power of 20 mW at 16-μm is obtained. However, because of the high efficiency, powerful performance, and well-developed technology, the CO_2 laser is an attractive candidate for the 16-μm light source. The 16-μm laser is obtained by using the transition between the (02^{0}0) and (01^{1}0) levels of the CO_2 molecules. However, since the lower laser level (01^{1}0) has very low energy, a number of CO_2 molecules, subject to the Boltzmann distribution defined by a given vibrational temperature, thermally populate this level. This reduces the population inversion between the laser levels resulting in the reduction of output power of the laser. The lower level population may be greatly reduced by cooling the CO_2 gas, which is indispensable

Submitted Aug. 20, 1983; revision received Aug. 21, 1984.

*Professor, Department of Aerospace Engineering.
†Senior Scientific Officer, Department of Aerospace Engineering.

in establishing population inversion between the (02^00) and (01^1) levels. In this regard, a gasdynamic laser scheme is the most promising candidate for the 16-μm laser source for two important reasons. First, in the gasdynamic laser (GDL), the lowering of the temperature at the laser cavity is realized quite easily by expanding the laser gas mixture through a nozzle of large area ratio. Second, a GDL can produce high power because of its high-saturation parameter.

There has been no experimental work reported on 16-μm GDLs except for the work reported in a series of papers by Stregack et al.,[6,7] Manuccia et al.,[8] and Wexler et al.[9,10] They reported the performance of a 16-μm CO_2 laser with an aftermixing-type electric discharge gasdynamic laser, where an N_2-He mixture is vibrationally excited by a glow discharge in the subsonic plenum and the gas mixture is then accelerated through an array of supersonic nozzles where cold CO_2 is injected. The vibrationally excited N_2 transfers all of its energy to populate the (00^01) level of CO_2 in this region, which may be utilized to establishing the population inversion between (02^00)-(01^10) levels by injecting an external laser signal at 9.4-μm into the laser cavity. However, the main drawback of this GDL system is that the extractable laser power is limited mainly by the capacity of the electrical discharge power supply as a power source. The best alternative in terms of specific extractable laser power is a conventional GDL operating at high reservoir pressure and temperature which can be achieved by combustion. There has been no experimental work reported on the conventional 16-μm GDL to date. Recently, however, the possibility of obtaining high-power 16-μm radiation from a conventional CO_2 GDL by theoretical simulation was evaluated by Suzuki et al.[11] and Saito et al.[12-14] For a GDL using a nozzle of large area ratio they showed that a maximum 16-μm gain of 2.5% cm^{-1} can be obtained for parameters with a reservoir temperature $T_0' = 1200$ K, reservoir pressure $p_0' = 15$ atm, gas mole fraction $CO_2{:}N_2{:}H_2 = 20{:}73{:}7(\%)$, a nozzle area ratio of 100.

It is evident from the existing literature on the conventional 10.6-μm and 16-μm CO_2 gasdynamic lasers that the performance characteristics of a GDL depend on too many parameters, e.g., reservoir temperature and pressure, gas composition, nozzle shape and size. Making an exhaustive study of the influence of these parameters on the GDL performance would indeed be very formidable. Even if a chosen set of operating conditions yields susbstantially good performance, it need not be the optimum obtained from the system. The aim of this paper is to obtain a completely generalized characterization of GDL performance in a formal way and to obtain a universal correlating parameter (combining all of the GDL parameters) that could be used to optimize the performance of the 16-μm gasdynamic CO_2 laser. Recently, the authors have completed work on the 10.6-μm CO_2-N_2-H_2O or He GDL using different nozzle shapes such as wedge, conical, and hyperbolic. They have employed similar techniques to study the 16-μm CO_2-N_2-H_2 laser herein.

Governing Equations

The vibrational energy levels used for 16 μm laser emission in CO_2 molecules are (02^00) and (01^10). To produce the population inversion between these two levels, the (001) level of CO_2 is fully populated at first, then an intense saturating laser pulse of 9.4-μm radiation is injected to depopulate the (001) level and populate the (02^00) level. The 9.4-μm laser pulse is chosen in such a way that it is intense and short enough to pump the (02^00) level within its de-excitation time. Then the transition between the (001) and (02^00) levels is saturated completely and their population becomes equal. Therefore, we can write,[11]

$$N_{02^00} = \tfrac{1}{2}(N'_{02^00} + N_{001})$$

The population of the lower laser level (01^10) is calculated by the Boltzmann distribution defined by the vibrational temperature.

Suzuki et al.[11] used a three-temperature vibrational energy model for the simulation of the 16-μm CO_2 GDL, as shown in Fig. 1a. In the present analysis, the authors have adopted a two-temperature model introduced by Anderson[15] as shown in Fig. 1b, where mode I (of vibrational temperature T_I') and mode II (of vibrational temperature T_{II}') represent the lower and upper levels of the laser's system, respectively. The net effect of various complex vibrational energy exchanges taking place due to molecular collisions is reduced in this model to the relaxation of mode II via τ_a' and τ_b' and the relaxation of mode I via τ_c'. The average relaxation times, τ_a', τ_b', and τ_c', are shown in Fig. 1b. The primes denote the dimensional quantities.

The two-temperature model is governed by the three global mass, momentum, and energy conservation equations, the equation of state, and the rate equations governing the vibrational relaxation of the two modes. These equations are normalized by using reservoir conditions and nozzle scale parameter L' and are given by

$$\rho u A = \text{const} \tag{1}$$

$$u\,du + (dp/\rho) = 0 \tag{2}$$

$$\tfrac{1}{2}u^2 + (1+\alpha)T + e_v = \text{const} \tag{3}$$

$$p = \rho T \tag{4}$$

and

$$u\frac{d(e_v)_i}{dx} = \frac{L'}{u_0'\tau_i'}[(e_v)_e - (e_v)]_i \quad i = \text{I,II} \tag{5}$$

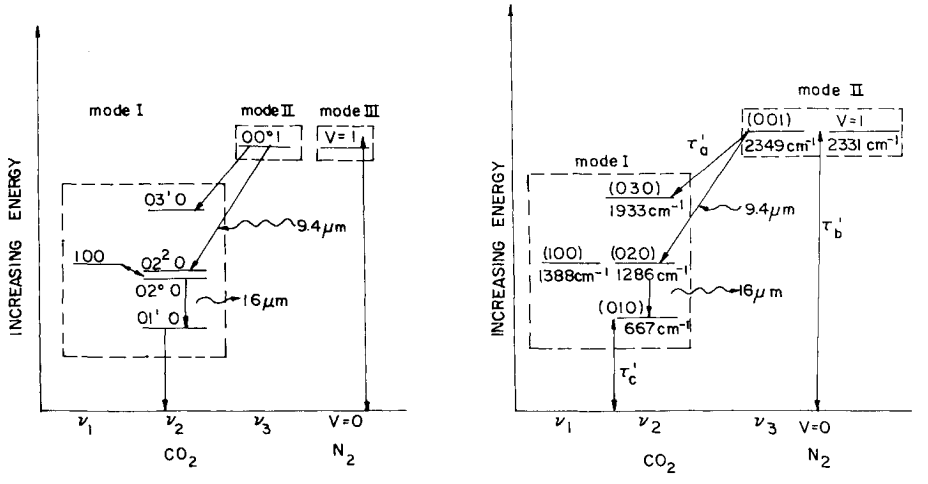

Fig. 1 Schematic of the vibrational models of a) Ref. 11 and b) Ref. 15.

where the normalized specific energies are given by

$$(e_v)_{\rm I} = X_{\rm C}\left[\frac{\theta_{v1}}{\exp(\theta_{v_1}/T_{\rm I})-1}+\frac{2\theta_{v2}}{\exp(\theta_{v_2}/T_{\rm I})-1}\right]$$

$$(e_v)_{\rm II} = X_{\rm C}\left[\frac{\theta_{v1}}{\exp(\theta_{v_3}/T_{\rm II})-1}+\frac{X_{\rm N}}{X_{\rm C}}\frac{\theta_{v_{\rm N}}}{\exp(\theta_{v_{\rm N}}/T_{\rm II})-1}\right] \tag{6a}$$

and

$$\alpha = 2.5(X_{\rm C}+X_{\rm N}+X_{\rm H}) \tag{6b}$$

In the above equations the pressure, density, energy, temperature, and velocity are normalized with respect to their reservoir conditions. In addition, a family of nozzles is considered whose normalized cross-sectional area A is given by

$$A = (1+x^j)^i \tag{7}$$

where $i=1, j=1$ for wedge nozzles, and $i=2, j=1$ for conical nozzles, and $i=1, j=2$ for hyperbolic nozzles.

Following the procedure given in detail in Ref. 16 the above equations are reduced to a similar form by defining a new independent variable η, which is a function of the normalized density; the solutions then depend only on two parameters. By transforming η to ξ (the latter variable being a function of the specific entropy and normalized density), the governing equations assume a universal form with the solutions depending only on a single parameter $\chi_{\rm I}$, which combines all of the other parameters of the problem. The universal governing equations in their final universal form for the 16-μm CO_2 GDL are

$$\psi - \alpha\frac{d\psi}{d\xi} - X_{\rm C}\left[\bar{G}_{\rm I}\frac{d\phi_{\rm I}}{d\xi}+\bar{G}_{\rm II}\frac{d\phi_{\rm II}}{d\xi}\right] = 0 \tag{8}$$

and

$$\frac{d\phi_{\rm I}}{d\xi} = \frac{K_{\rm I}\psi}{N_s}\exp\left[\chi_{\rm I}+\xi\left(1-\frac{1}{ij}\right)-B_{\rm CC}\psi^{-1/3}\right]\left(\frac{\bar{E}_e-\bar{E}}{\bar{G}}\right)_{\rm I} \tag{9a}$$

$$\frac{d\phi_{\rm II}}{d\xi} = \frac{K_{\rm II}\psi}{N_s}\exp\left[\chi_{\rm II}+\xi\left(1-\frac{1}{ij}\right)-B_{\rm NN}\psi^{-1/3}\right]\left(\frac{\bar{E}_e-\bar{E}}{\bar{G}}\right)_{\rm II} \tag{9b}$$

Equation (8) is the generalized momentum equation obtained by combining the momentum and energy equations and the equation of state. Equations (9a) and (9b) are the rate equations governing the relaxation of vibrational energies of modes I and II, respectively. The nonequilibrium solutions of these equations are used to calculate the population inversion (PI) and the small signal gain (G_0) downstream from nozzle throat. For the homogeneously broadened $P(15)$ (02^00) $\rightarrow(01^10)$ transitions at a wavelength of 16-μm the population inversion and the small signal gain as functions of the flow quantities are given by the following algebraic equations:

$$\mathrm{PI} = \frac{\tfrac{1}{2}\exp(-\theta_{v_3}/\phi_{\rm II}) - [2-(3/2)\exp(-\theta_{v_2}/\phi_{\rm I})]\exp(\theta_{v_2}/\phi_{\rm I})}{Q_{\rm vib}} \tag{10}$$

and

$$G_0 = 0.168\frac{(\mathrm{PI})}{P(X_i)\psi^{3/2}}\exp(-0.04012/\psi) \tag{11}$$

where

$$Q_{\rm vib} = [1-\exp(-\theta_{v_1}/\phi_{\rm I})]^{-1}[1-\exp(-\theta_{v_2}/\phi_{\rm I})]^2 \times [1-\exp(-\theta_{v_3}/\phi_{\rm II})]^{-1} \tag{12}$$

and

$$P(X_i) = 1+0.7589(X_{\rm N}/X_{\rm C})+1.0695(X_{\rm H}/X_{\rm C}) \tag{13}$$

The variables are defined as $\psi = T'/\theta'_{v_{\rm N}}$, $\phi_{\rm I} = T'_{\rm I}/\theta'_{v_{\rm N}}$, and $\phi_{\rm II} = T'_{\rm II}/\theta'_{v_{\rm N}}$, where $\theta'_{v_{\rm N}} = 3357$ K. The characteristic temperatures $\theta'_{v_1} = 1999$ K, $\theta'_{v_2} = 960$ K, and $\theta'_{v_3} = 3393$ K of the three vibrational modes of CO_2 are also normalized with respect to $\theta'_{v_{\rm N}}$. The independent variable ξ in Eqs. (8) and (9) is a function of the normalized density $\rho = \rho'/\rho'_0$, and specific entropy S_0, defined as

$$\xi = S_0 + \ell n(\rho) \tag{14}$$

The initial values for solving Eqs. (8) and (9) for nonequilibrium solutions downstream of the throat are obtained from the vibrational-equilibrium solutions of these equations. Equilibrium occurs when the vibrational relaxation times τ are very small. Then, rate equations (9) yield $\psi = \phi_{\rm I} = \phi_{\rm II} = \psi^e$. From these equilibrium solutions an expression for the specific entropy is obtained.

$$S_0 = -\ell n\rho^e + \alpha\ell n\psi^e + \frac{X_{\rm C}}{\psi^e}[\bar{E}_{\rm I}+\bar{E}_{\rm II}]_e - X_{\rm C}\ell n\{[1-\exp(-\theta_{v_1}/\psi)][1-\exp(-\theta_{v_2}/\psi)]^2 \times [1-\exp(-\theta_{v_3}/\psi)][1-\exp(-1/\psi)]^{(X_{\rm N}/X_{\rm C})}\}_e + S_r \tag{15}$$

where the reference entropy S_r is a constant equal to 28.63 for H_2 diluent in the CO_2-N_2 GDL using conical and hyperbolic nozzle shapes ($ij=2.0$).

Following are the various other factors occurring in the above equations.

$$\bar{E}_{\rm I} = \frac{\theta_{v1}}{\exp(\theta_{v_1}/\phi_{\rm I})-1}+\frac{2\theta_{v2}}{\exp(\theta_{v_2}/\phi_{\rm I})-1} \tag{16a}$$

$$\bar{E}_{\rm II} = \frac{\theta_{v3}}{\exp(\theta_{v_3}/\phi_{\rm II})-1}+\frac{X_{\rm N}/X_{\rm C}}{\exp(1/\phi_{\rm II})-1} \tag{16b}$$

$$\bar{G}_{\rm I} = \left(\frac{\theta_{v1}}{\phi_{\rm I}}\right)^2\frac{\exp(\theta_{v_1}/\phi_{\rm I})}{[\exp(\theta_{v_1}/\phi_{\rm I})-1]^2} + 2\left(\frac{\theta_{v2}}{\phi_{\rm I}}\right)^2\frac{\exp(\theta_{v_2}/\phi_{\rm I})}{[\exp(\theta_{v_2}/\phi_{\rm I})-1]^2} \tag{17a}$$

$$\bar{G}_{\rm II} = \left(\frac{\theta_{v3}}{\phi_{\rm II}}\right)^2\frac{\exp(\theta_{v_3}/\phi_{\rm II})}{[\exp(\theta_{v_3}/\phi_{\rm II})-1]^2} + \frac{X_{\rm N}}{X_{\rm C}}\frac{1}{\phi_{\rm II}^2}\frac{\exp(1/\phi_{\rm II})}{[\exp(1/\phi_{\rm II})-1]^2} \tag{17b}$$

$$K_{\rm I} = X_{\rm C}+X_{\rm N}[(\tau'_c)_{\rm CC}/(\tau'_c)_{\rm CN}]+X_{\rm H}[(\tau'_c)_{\rm CC}/(\tau'_c)_{\rm CH}] \tag{18a}$$

$$K_{\rm II} = [X_{\rm N}K_b + X_{\rm C}K_a(\tau'_b)_{\rm NN}/(\tau'_a)_{\rm CC}]/(X_{\rm C}+X_{\rm N}) \tag{18b}$$

where

$$K_a = X_{\rm C}+X_{\rm N}[(\tau'_a)_{\rm CC}/(\tau'_a)_{\rm CN}]+X_{\rm H}[(\tau'_a)_{\rm CC}/(\tau'_a)_{\rm CH}] \tag{19a}$$

$$K_b = X_{\rm C}[(\tau'_b)_{\rm NN}/(\tau'_b)_{\rm NC}]+X_{\rm N}+X_{\rm H}[(\tau'_b)_{\rm NN}/(\tau'_b)_{\rm NH}] \tag{19b}$$

The vibrational relaxation times for various collisional partners are given in the Appendix.

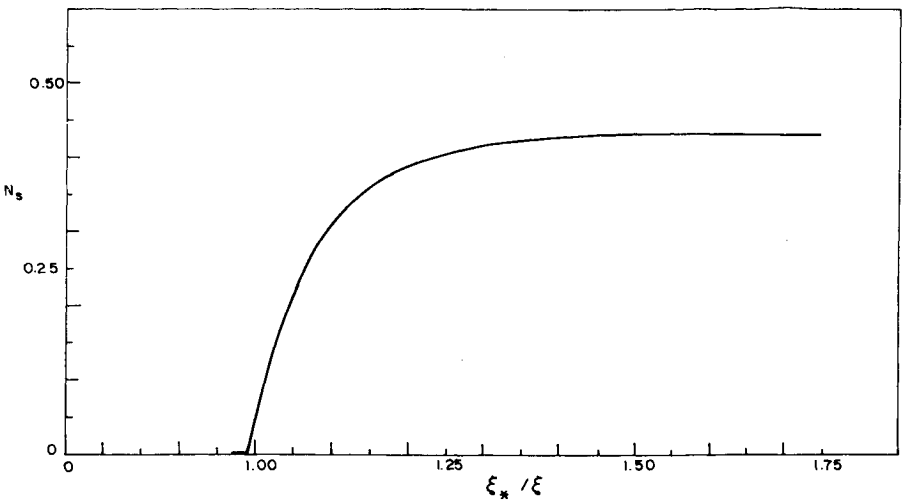

Fig. 2 Function N_s for CO_2-N_2-H_2 gas mixture.

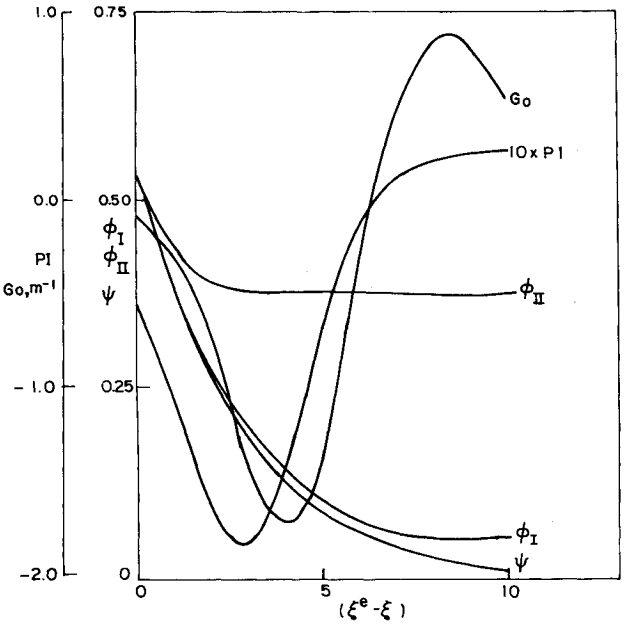

Fig. 3 Variation of flow quantities downstream of the nozzle throat for $X_{CO_2} = 0.025$, $X_{N_2} = 0.905$, $X_{H_2} = 0.07$, $ij = 2.0$, $\chi_I = -6.5$, $\psi^e = 0.625$, and $\xi^e = 27.696$.

The parameter χ in Eqs. (9) is a universal parameter that combines all other system parameters such as reservoir pressure p_0', reservoir temperature T_0', mixture gas constant R_M', normalized density ρ and velocity u at the throat, and the nozzle shape parameter $L' = r_*'/\tan(\delta)$. The parameter χ for modes I and II (which may be called a universal gasdynamic parameter) is given by

$$\chi_I = \ell n\left[\frac{p_0' L' \theta_{\nu_N}' (\rho_* u_*)^{6+1/ij}}{ij R_M'^{1/2} T_0'^{3/2} J_{CC}}\right] - (1 - 1/ij) S_0 \qquad (20a)$$

and

$$\chi_{II} = \ell n\left[\frac{p_0' L' \theta_{\nu_N}' (\rho_* u_*)^{6+1/ij}}{ij R_M'^{1/2} T_0'^{3/2} J_{NN}}\right] - (1 - 1/ij) S_0 \qquad (20b)$$

where $\rho_* u_*$ is the nondimensional critical mass flow. Constants B and J in Eqs. (9) and (20) are calculated from the vibrational relaxation times and are independent of the diluent used. The values of these constants are as follows:

$$B_{CC} = 2.7389, \quad J_{CC} = 1.555 \times 10^{-8} \text{ atm-s}$$

$$B_{NN} = 14.3098, \quad J_{NN} = 2.45 \times 10^{-11} \text{ atm-s}$$

The function N_S in Eqs. (9) is a nonsimilar function, and for any given nozzle shape a function of local velocity, Mach number, and nozzle area ratio, and given by

$$N_s = \mp (M^2/M^2 - 1)(1 - A^{-1/i})^{(j-1)/j} u^{1+1/ij} (\rho_* u_*)^6 \qquad (21)$$

where the minus sign is valid for $M < 1$ and the plus sign for $M > 1$. Since M, u, and A vary with ξ, the nonsimilar function N_s is also a function of ξ. The variation of N_s as a function of ξ for a CO_2-N_2-H_2 mixture flow in a conical or hyperbolic nozzle is generated using the computer program of Lordi et al.[17] Figure 2 shows the function N_s for GDL mixtures. Further details of the computation of N_s are given in Ref. 18. The N_s curve for the CO_2-N_2-H_2 gas mixture flow in a conical or hyperbolic nozzle is represented by the following analytical expression:

$$\begin{aligned} N_s &= 0.0, && \text{for } \xi_*/\xi \le 0.988 \\ &= 0.03 - 12.5(0.995 - \xi_*/\xi)^{0.45}, && \text{for } 0.988 < \xi_*/\xi \le 0.995 \\ &= 0.431 - 1.72 \times 10^4 (\xi_*/\xi + 0.7)^{-20.2}, && \text{for } \xi_*/\xi > 0.995 \end{aligned} \qquad (22)$$

If the function $N_s = 0$, then the flow is in vibrational equilibrium, and if $N_s > 0$ then nonequilibrium flow exists in the nozzle.

Similarly the mass flow factor $(\rho_* u_*)$ and the density ρ_* have been computed as functions of the reservoir temperature and are found to be independent of reservoir temperature. These functions have the constant values

$$\rho_* u_* = k_1 = 0.6638 = \text{const} \qquad (23)$$

$$\rho_* = k_2 = 0.6288 = \text{const} \qquad (24)$$

In addition, the normalized velocity ratio (u/u_*) along the conical or hyperbolic nozzle has been correlated as a function of the normalized area ratio $A = A'/A_*'$, using the computer program of Ref. 17 and given by

$$\left(\frac{u}{u_*}\right) k_1^{7.183} = [-0.0036 + 0.0635(0.652 + \log_{10} A)^{-3.176}] \quad \text{for } M < 1.0 \qquad (25)$$

$$\left(\frac{u}{u_*}\right) k_I^{7.183} = [0.706 - 0.1925(0.202 + \log_{10} A)^{-0.548}] \quad \text{for } M \geq 1.0 \qquad (26)$$

The main objective is to solve Eqs. (8) and (9) for variables ψ, ϕ_I, and ϕ_{II} which are then used in Eqs. (10) and (11) to obtain population inversion and the optical gain G_0 of the 16-μm gasdynamic CO_2 laser. From inspection of Eqs. (8) and (9) it is clear that, for a given gas mixture and a value of ij, the solutions of these equations depend on a single parameter χ_I, since

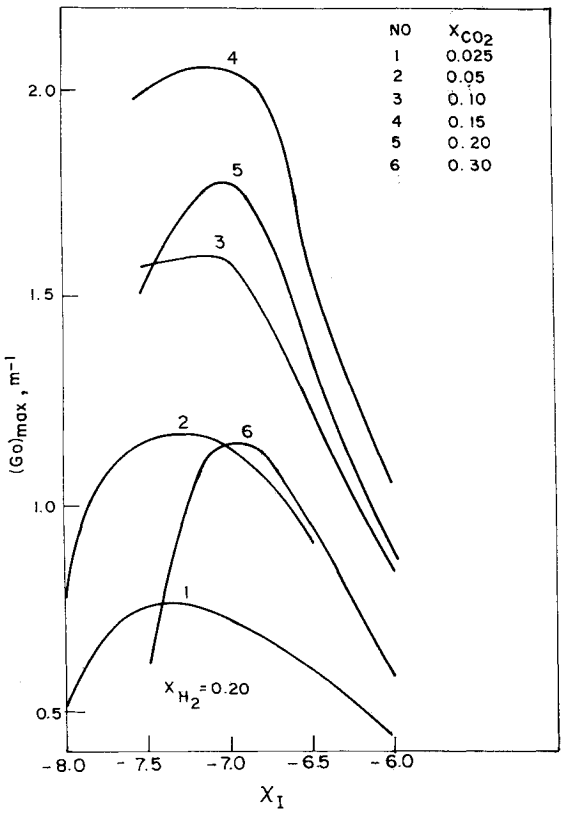

Fig. 4 Variation of maximum values of small signal gain on the $P(15)(02^00)-(01^10)$ transition with χ_I for various mixture compositions of 16-μm CO_2-N_2-H_2 gasdynamic laser.

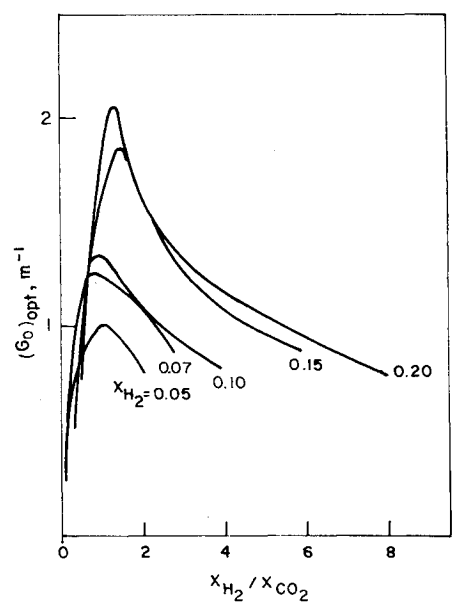

Fig. 5 Effect of ratio of mole fraction of H_2 and CO_2 on optimum small signal gain.

χ_{II} differs from χ_I by a constant factor. It is apparent that χ_I combines all other system parameters. In this sense the solutions obtained here are universal.

Results and Discussion

Equations (8) and (9) are solved for the unknowns ψ, ϕ_I, and ϕ_{II} simultaneously for a given laser gas mixture and $ij = 2.0$ (a family of conical or hyperbolic nozzles) with χ as a parameter. The detailed procedure for solving these equations is given in Ref. 19. Computations are carried out for a wide range of mixture compositions, for the H_2 mole fraction varying from 5 to 20%, with the CO_2 mole fraction varying from 2.5 to 30% for each H_2 mole fraction. For each case the variations of ψ, ϕ_I, and ϕ_{II}, and the corresponding values of PI and G_0, are computed along the nozzle. These solutions are shown in Fig. 3 for a sample case. As in the case of a 10.6-μm laser, the 16-μm laser also shows the tendency of G_0 to attain a maximum while PI remains constant far downstream of the throat. Such peak values of G_0 are obtained for each composition over a wide range of values of χ_I. Figure 4 shows the variation of maximum G_0 for a sample set of composition with a H_2 mole fraction of 20%. From these plots it is shown that for every gas mixture G_0 attains a maximum at a particular value of χ_I. These two quantities are designated as $(G_0)_{opt}$ and $(\chi_I)_{opt}$, respectively, which are the optimum values. Thus, for a given laser gas composition, $(G_0)_{opt}$ represents the highest possible value of small signal gain that could be achieved. For example, the optimum value of small signal gain for the composition CO_2:N_2:H_2 = 15:65:20(%) in a GDL using a conical or hyperbolic nozzle oscillating at 16-μm is 2.06% cm^{-1} and the corresponding optimum value of χ_I is -7.1. The influence of the CO_2 and H_2 contents on the optimum values of G_0 is shown in Fig. 5. This figure shows that for a given H_2 content, $(G_0)_{opt}$ attains a maximum at some value of CO_2 mole fraction and this maximum value increases with increasing value of H_2 mole fraction.

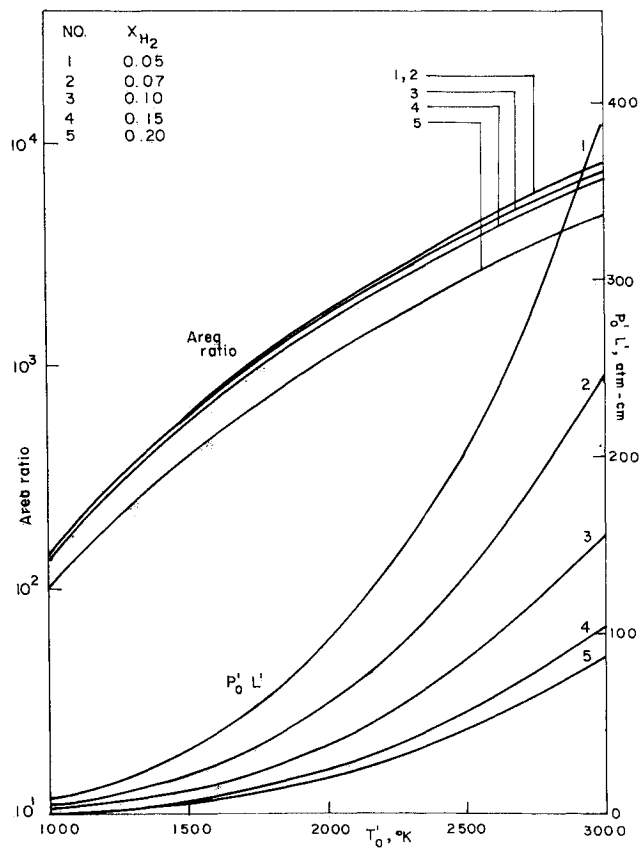

Fig. 6 Variation of optimum area ratio and $p_0'L'$ with reservoir temperature for $ij = 2.0$ and $X_{CO_2} = 0.20$.

After obtaining the optimum values of G_0 and χ_I for any given laser gas mixture, the optimum operating conditions, such as the reservoir temperature T_0' and pressure p_0', can be readily computed. Since the universal parameter χ_I, as given in Eqs. (20), is a function of T_0' and p_0' with L', the nozzle shape factor, as a parameter, the values for the binary parameter $p_0'L'$, can be calculated as a function of T_0'. The binary parameter $p_0'L'$ is than plotted as a function of T_0'. These plots are used for computing p_0' as a function of T_0' for any chosen value of L'. The variation of $p_0'L'$ with T_0' is shown in Fig. 6 as a sample case.

The optimum area ratio corresponding to the optimum reservoir conditions which would yield an optimum value of small signal gain can be computed using the following equation. For the given nozzle (i.e., *ij*) and gas composition, and for the graphically known value of χ_I, the governing equations are solved to obtain the maximum value of G_0 (which will also be the optimum value) and the corresponding value of ξ (designated as ξ_{opt}). Using Eqs. (14) and (26) it is shown that the optimum area ratio A_{opt} and ξ_{opt} are related by the following equation:

$$[0.706-0.1925(0.202+\log_{10}A_{opt})^{-0.548}]A_{opt} = k_1^{7.783}k_2\exp(S_0-\xi_{opt}) \quad (27)$$

where k_1, k_2, and S_0 are defined in Eqs. (23), (24), and (15), respectively. Since k_1, k_2, and S_0 are functions of T_0' only, the above equation can be solved for A_{opt} as a function of T_0' for a known value of ξ_{opt}. The values thus obtained for A_{opt} are plotted against T_0', which are shown in Fig. 6 as a sample case.

Conclusions

The universal governing equations for gas flows in 16-μm CO_2 gasdynamic lasers employing conical or hyperbolic nozzles have been presented. The solutions of these equations depend on a single parameter χ_I, which contains all of the other parameters of the problem. The solutions of the governing equations are used to compute the optimum values of small signal gain coefficient for the 16-μm operation and the corresponding values of the universal correlating parameter χ_I. The results are presented in graph form for a wide range of laser mixture composition. The optimum values of the area ratio and the binary scaling parameter $p_0'L'$ are computed as functions of reservoir temperature T_0' from these results. These optimum values are presented in graph form as well. In the present analysis it has been shown that for a gas composition of CO_2:N_2:H_2 = 15:65:20(%), a gain of up to 2.06% cm^{-1} can be achieved on the $P(15)$ $(02^00)\rightarrow(01^10)$ transition of CO_2 in a CO_2-N_2-H_2 laser system.

Appendix: Vibrational Relaxation Times for the CO_2-N_2-H_2 System

The expressions for the relaxation times τ_a', τ_b', and τ_c' for various collisional partners, taken from Refs. 11 and 15, are as follows:

$$(p'\tau_a')_{CO_2\text{-}N_2} = 1.3\times10^5[(T')^{-1/3}]^{4.9}$$

$$(p'\tau_a')_{CO_2\text{-}CO_2} = 0.27(p'\tau_a')_{CO_2\text{-}N_2}$$

$$(p'\tau_a')_{CO_2\text{-}H_2} = 0.7326+9.783\times10^{-6}[(T')^{-1/3}]^{4.861}$$

$$\log(p'\tau_b')_{N_2\text{-}N_2} = 93(T')^{-1/3}-4.61$$

$$(p'\tau_b')_{N_2\text{-}CO_2} = (p'\tau_b')_{N_2\text{-}N_2}$$

$$\log(p'\tau_b')_{N_2\text{-}H_2} = -1.3137+50.487[(T')^{-1/3}]^{1.413}$$

$$\log(p'\tau_c')_{CO_2\text{-}CO_2} = 17.8(T')^{-1/3}-1.808$$

$$(p'\tau_c')_{CO_2\text{-}N_2} = 2(p'\tau_c')_{CO_2\text{-}CO_2}$$

$$\log(p'\tau_c')_{CO_2\text{-}H_2} = 9.247-14.482[(T')^{-1/3}]^{0.142}$$

In the above relations, $(p'\tau')$ is in atm-μs and the translational temperature T' is in degrees Kelvin.

Acknowledgment

This research was supported by the Aeronautical Research and Development Board of the Government of India.

References

[1]Osgood, R. M. Jr., "Optically Pumped 16-μm CO_2 Laser," *Applied Physics Letters*, Vol. 28, March 1976, pp. 342-345.

[2]Tiee, J. J. and Witling, C., "CF_4 and NOCl Molecular Lasers Operating in the 16-μm Region," *Applied Physics Letters*, Vol. 30, April 1977, pp. 420-422.

[3]Baranov, V. Yu, et al., "Pulse-Periodic of an Optically Pumped CF_4 Laser with an Average Output Power of 0.2 W," *Soviet Journal of Quantum Electronics*, Vol. 8, April 1978, pp. 544-546.

[4]Byer, R. L., "A 16-μm Source for Laser Isotope Enrichment," *IEEE Journal of Quantum Electronics*, Vol. QE-12, Nov. 1976, pp. 732-733.

[5]Rabinowitz, P., Stein, A., Brickman, R., and Kaldor, A., "Efficient Tunable H_2 Raman Laser," *Applied Physics Letters*, Vol. 35, Nov. 1979, pp. 739-741.

[6]Stregack, J. A., Wexler, B. L., and Hart, G. A., "D_2-CO_2 and D_2-N_2O Electric Discharge Gas-Dynamic Lasers," *Applied Physics Letters*, Vol. 27, Dec. 1975, pp. 670-671.

[7]Stregack, J. A., Wexler, B. L., and Hart, G. A., "CW CO-CS_2, CO-C_2H_2 and CO-N_2O Energy Transfer Lasers," *Applied Physics Letters*, Vol. 28, Feb. 1976, pp. 137-139.

[8]Manuccia, T. J., Stregack, J. A., Harris, N. W., and Wexler, B. L., "14- and 16-μm Gasdynamic CO_2 Lasers," *Applied Physics Letters*, Vol. 29, Sept. 1976, pp. 360-362.

[9]Wexler, B. L., Manuccia, T. J., and Waynant, R. W., "CW and Improved Pulsed Operation of the 14- and 16-μm CO_2 Lasers," *Applied Physics Letters*, Vol. 31, Dec. 1977, pp. 730-732.

[10]Wexler, B. L. and Waynant, R. W., "High-Average-Power 16-μm Gasdynamic CO_2 Laser Using a Multipass Cavity," *Applied Physics Letters*, Vol. 34, May 1979, pp. 674-677.

[11]Suzuki, K., Saito, S., Obara, M., and Fujioka, T., "Theoretical Study for a 16-μm CO_2 Gasdynamic Laser," *Journal of Applied Physics*, Vol. 51, Aug. 1980, pp. 4003-4009.

[12]Saito, S., Suzuki, K., Obara, M., and Fujioka, T., "Theoretical Analysis of 16-μm CO_2 Gasdynamic Laser," *Journal of Physics*, Vol. 41, Nov. 1980, pp. 167-173.

[13]Saito, S., Obara, M., and Fujioka, T., "Theoretical Characteristics of 16-μm CO_2 Gasdynamic Laser," *Journal of Applied Physics*, Vol. 52, July 1981, pp. 4422-4428.

[14]Saito, S., Obara, M., and Fujioka, T., "Computer Simulation of CW 16-μm CO_2 Gasdynamic Lasers," *Applied Optics*, Vol. 20, Aug. 1981, pp. 2838-2842.

[15]Anderson, J. D. Jr., "Time-Dependent Analyses of Population Inversions in an Expanding Gas," *The Physics of Fluids*, Vol. 13, Aug. 1970, pp. 1983-1989.

[16]Reddy, N. M. and Shanmugasundaram, V., "Theoretical Gain-Optimization Studies in CO_2-N_2 Gasdynamic Lasers. I. Theory," *Journal of Applied Physics*, Vol. 50, April 1979, pp. 2565-2575.

[17]Lordi, J. A., Mates, R. E., and Moselle, J. R., "Computer Program for the Numerical Solution of Nonequilibrium Expansions of Reacting Gas Mixtures," NASA CR-492, May 1966.

[18]Reddy, K.P.J. and Reddy, N. M., "Theoretical Gain Optimization Studies in 10.6 μm CO_2-N_2 Gasdynamic Lasers, IV. Further Results of Parametric Study," *Journal of Applied Physics*, Vol. 55, Jan. 1984, pp. 51-59.

[19]Reddy, N. M. and Shanmugasundaram, V., "Gain-Optimization Studies in CO_2-N_2 Gas Dynamic Lasers," *Gas-Flow and Chemical Lasers*, edited by J. F. Wendt, 1978, pp. 319-328.